ELSEVIER

Journal of Alloys and Compounds 452 (2008) 359–366

Journal of ALLOYS AND COMPOUNDS

www.elsevier.com/locate/jallcom

# Formation of icosahedral phase in $Zr_{65}Al_{7.5}Ni_{10}Cu_{12.5}Ag_5$ metallic glass

Z.J. Yan *, S.E. Dang, Q.S. Li, W.X. Hao, Y. Hu

*School of Materials Science and Engineering, Taiyuan University of Science and Technology, Taiyuan 030024, PR China*

Received 29 September 2006; received in revised form 17 November 2006; accepted 17 November 2006
Available online 15 December 2006

**Abstract**

Two $Zr_{65}Al_{7.5}Ni_{10}Cu_{12.5}Ag_5$ amorphous specimens were prepared from the mother ingots with different solidification microstructures. Observation by high-resolution electron microscopy (HREM) revealed that there existed numerous nano-sized short-range order regions (SRORs) in the as-cast specimens although their amorphous nature had been verified by X-ray diffraction (XRD). The average size of the SRORs decreased significantly as the solidification microstructure of the mother ingot became finer. The transformation from amorphous to icosahedral phase (I-phase) in the $Zr_{65}Al_{7.5}Ni_{10}Cu_{12.5}Ag_5$ metallic glass was systematically investigated by differential scanning calorimetry (DSC) under isochronal and isothermal conditions. The results indicated that the transformation kinetics slightly changed, and that the formation of I-phase was triggered by the growth of those SRORs as the pre-existing embryos. It was strongly suggested that the atomic configuration of the unit structure in the metallic glasses showed an icosahedron-like one.


*Keywords:* Icosahedral phase; Quasicrystals; Metallic glasses; Phase transformation

## 1. Introduction

The amorphous atomic configuration is a long-standing issue in solid-state physics and materials science [1–5]. Attempts to understand the properties of metallic glasses have resulted in the creation of some structural models, of which the most successful one is the polytope model [6]. The polytope model derives from the hypothesis that an icosahedron has the lowest energy for all kinds of clusters consisting of 13 atoms if atomic interactions according to a Lennard–Jones potential are assumed. The discovery of icosahedral phase (I-phase) in rapidly quenched $Al_{86}Mn_{14}$ shows the existence of the icosahedral configuration [7]. Later, molecular dynamic computer calculations based on empirical potentials further indicate that the icosahedral structures prevail in supercooled liquids [8,9]. Within the frame of energy landscape, the inherent structures of metallic glasses are the same as that of supercooled liquids [10], which implies that the amorphous structure is similar to the supercooled liquid. Recently, experimental results indicate the prevailing of the five-fold symmetry in the supercooled liquids and metallic glasses [11–14], which may well be attributable to the presence of embryos of I-phase. However, there is no direct experimental evidence for this aspect.

Since I-phase precipitates as the product of phase transformation during the cooling of some liquid alloys, the understanding of the formation mechanism of I-phase will help to understand the structure correlation between the pre- and post-transformation phases of supercooled liquids [15,16]. It is somewhat a pity that the cooling rate of liquid alloys is generally too quick to provide an experimental time window for investigation. It has been found that I-phase reproducibly precipitates as the primary phase during the crystallization of some metallic alloys, such as Zr–Al–Ni–Cu–NM (NM = Ag, Pd, Au, Pt) and Zr–Al–Ni–M (M = Pd, Au, Pt) multicomponent metallic alloys [17–19]. Furthermore, the I-phase shows high thermal stable against decomposition during a relatively broad temperature span, which provides an accessible experimental time and temperature window to investigate the phase transformation mechanism.

In the present work, $Zr_{65}Al_{7.5}Ni_{10}Cu_{12.5}Ag_5$ amorphous specimens with different microstructure were prepared first. Then their kinetics of transformation from amorphous to icosahedral phase was investigated by differential scanning calorimetry (DSC) under isochronal and isothermal conditions,

* Corresponding author.
*E-mail address:* yanzhijie74@sohu.com (Z.J. Yan).

0925-8388/$ – see front matter © 2006 Elsevier B.V. All rights reserved.
doi:10.1016/j.jallcom.2006.11.093

through which the formation mechanism of I-phase was revealed.

## 2. Experimental

Two ingots with a nominal composition of $Zr_{65}Al_{7.5}Ni_{10}Cu_{12.5}Ag_5$ (at%) were prepared by arc melting the mixture of pure metals Zr (99.9 wt%), Al (99.99 wt%), Ni (99.9 wt%), Cu (99.99 wt%) and Ag (99.9 wt%) in a water-cooled copper crucible under titanium-gettered argon atmosphere. To enhance the composition homogeneity, the two original ingots were all repeatedly melted for 4 times at 1300 K first, and the resultant ingots were marked with A0. Then, one ingot A0 was further repeatedly melted for 12 times at 1580 K (marked with A12). The time of each melting operation was 60 s. The temperatures of melts under the definite conditions (i.e., the fixed weight of ingot, arc melting current and height of the tungsten electrode) were measured using the Pt–Ru (type B) thermocouple coated with quartz tube, being embedded in the melts. The experiments showed the precision of the temperatures measurement can be controlled within ±10 K. Under the same cooling conditions, two specimens with a cross section of 1 mm × 10 mm and length of 50 mm were produced from these ingots by suction casting in a copper mold. The specimens cast from the ingots A0 and A12 were marked with G0 and G12, respectively. The amorphous nature of the as-cast specimens and the crystallized phases after annealing were identified by X-ray diffraction (XRD) using Cu Kα radiation (Rigaku Dmax-rc). The amorphous structure of the as-cast samples and the morphologies of icosahedral quasicrystals were observed by high-resolution electron microscopy (HREM, JEM-2010) operated at 200 kV. The kinetics of amorphous-to-icosahedral (AI) phase transformation was investigated by DSC under isochronal (NETZCH DSC 404) and isothermal (Perkin-Elmer Pyris Diamond) conditions. In the case of isochronal conditions, the DSC plots were recorded at the scanning rates of 10, 20, 30 and 40 K/min. During the isothermal annealing, the amorphous samples were firstly heated to the preset annealing temperatures (683, 688, 693 or 698 K) at a heating rate of 200 K/min, and then held for a certain period of time until the completion of AI transformation. Al and $Al_2O_3$ pans were utilized during the isothermal and isochronal conditions, respectively.

## 3. Results

### 3.1. Short-range order regions in the metallic glass

The results of chemical composition analysis indicated that the compositions of the ingots did not change after the repeated arc melting, excluding the influence of the variation of compositions, especially the content of oxygen, on the subsequent amorphous structure and the phase transformation kinetics. Fig. 1 shows the solidification microstructures of the ingots A0 and A12. The microstructure of A12 is obviously much finer than that of A0. The as-cast samples G0 and G12 were verified to be a single amorphous phase by the XRD patterns (Fig. 2). The HREM images of the as-cast samples G0 and G12 (Fig. 3), however, show that there exist nano-sized SRORs with fringe-like contrast features enclosed by the white loops. It can be clearly seen that the atomic configuration in the glass G12 is more random than that in G0. Furthermore, the average size of the SRORs in the glass G12 (about 3 nm) is much smaller that of G0 (about 6 nm). From the images of Figs. 1 and 3, it can be clearly seen that there exists a close relation between the solidification microstructure of the mother ingot and the corresponding amorphous structure. The finer ingot microstructure results in a more homogeneous atomic configuration. Here we are interested in the role of these SRORs in the formation of I-phase, which is expected to help to understand the atomic configuration of the amorphous structure.

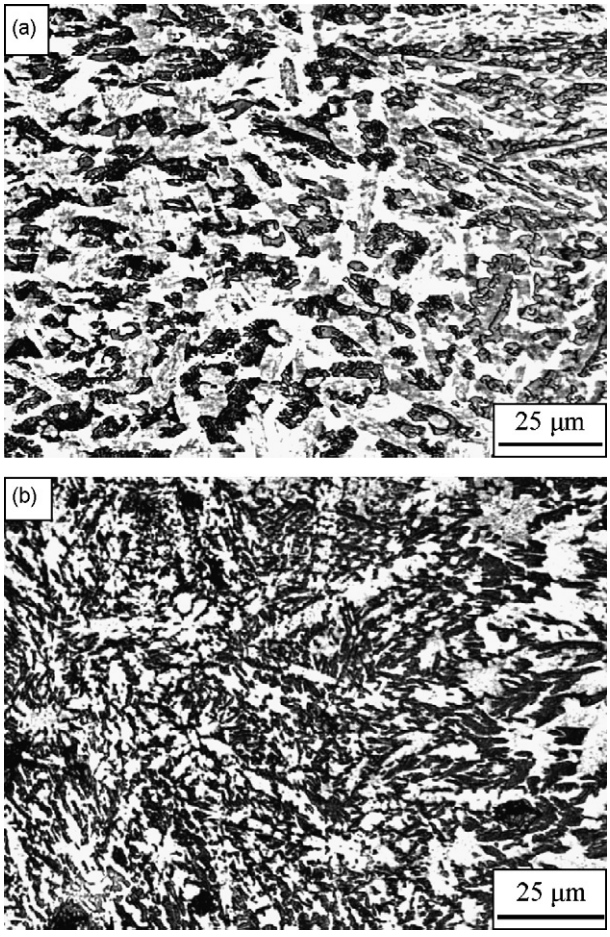


Fig. 1. Solidification microstructures of the mother ingots A0 (a) and A12 (b).

### 3.2. Transformation kinetics under isochronal conditions

The isochronal DSC plots of the glasses G0 and G12 recorded at the scanning rates of 10, 20, 30 and 40 K/min are shown in Fig. 4, and the detailed DSC data are shown in Tables 1 and 2, respectively. All the DSC curves show an endothermic event,

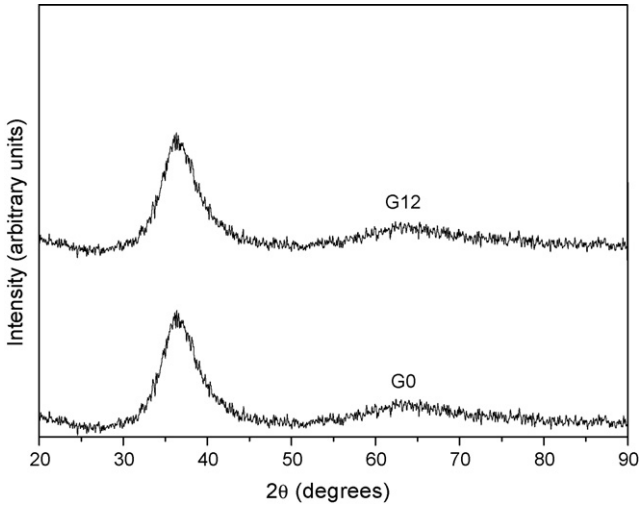


Fig. 2. XRD patterns of the as-cast samples G0 and G12.

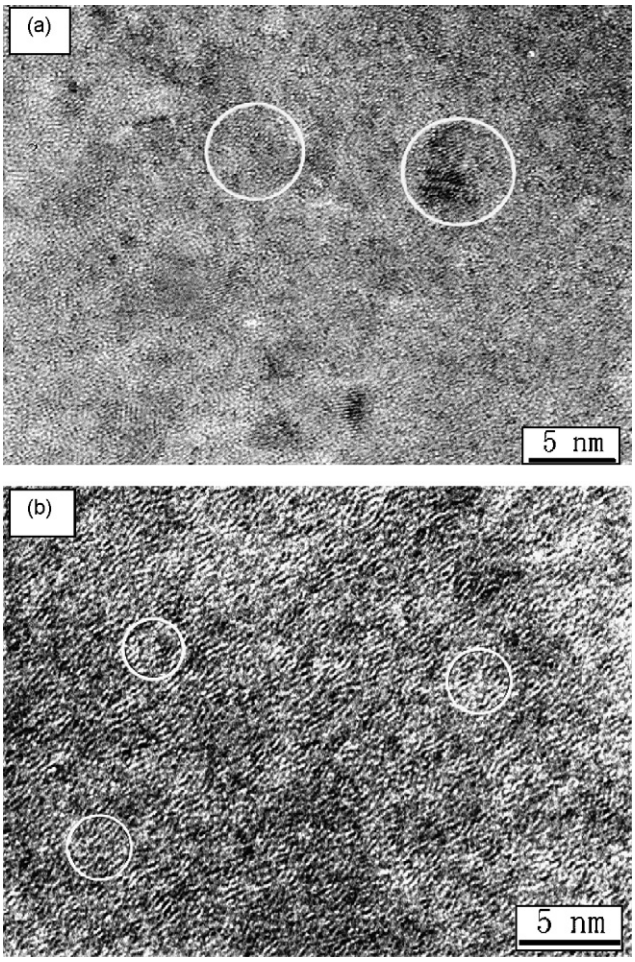


Fig. 3. HREM images of the amorphous samples G0 (a) and G12 (b).

Table 1
DSC data of the glass G0 recorded under isochronal conditions

| | Scanning rate, $\beta$ (K/min) | | | |
|---|---|---|---|---|
| | 10 | 20 | 30 | 40 |
| Glass transition temperature, $T_g$ (K) | 632.8 | 637.2 | 641.9 | 645.7 |
| Onset temperature of I-phase precipitation, $T_{x1}$ (K) | 696.2 | 711.9 | 722.5 | 731.0 |
| Onset temperature of I-phase decomposition, $T_{x2}$ (K) | 733.0 | 744.5 | 753.4 | 757.2 |

Table 2
DSC data of the glass G12 recorded under isochronal conditions

| | Scanning rate, $\beta$ (K/min) | | | |
|---|---|---|---|---|
| | 10 | 20 | 30 | 40 |
| Glass transition temperature, $T_g$ (K) | 634.3 | 639.3 | 644.7 | 647.8 |
| Onset temperature of I-phase precipitation, $T_{x1}$ (K) | 699.5 | 711.9 | 722.7 | 731.4 |
| Onset temperature of I-phase decomposition, $T_{x2}$ (K) | 738.8 | 745.2 | 754.5 | 758.2 |

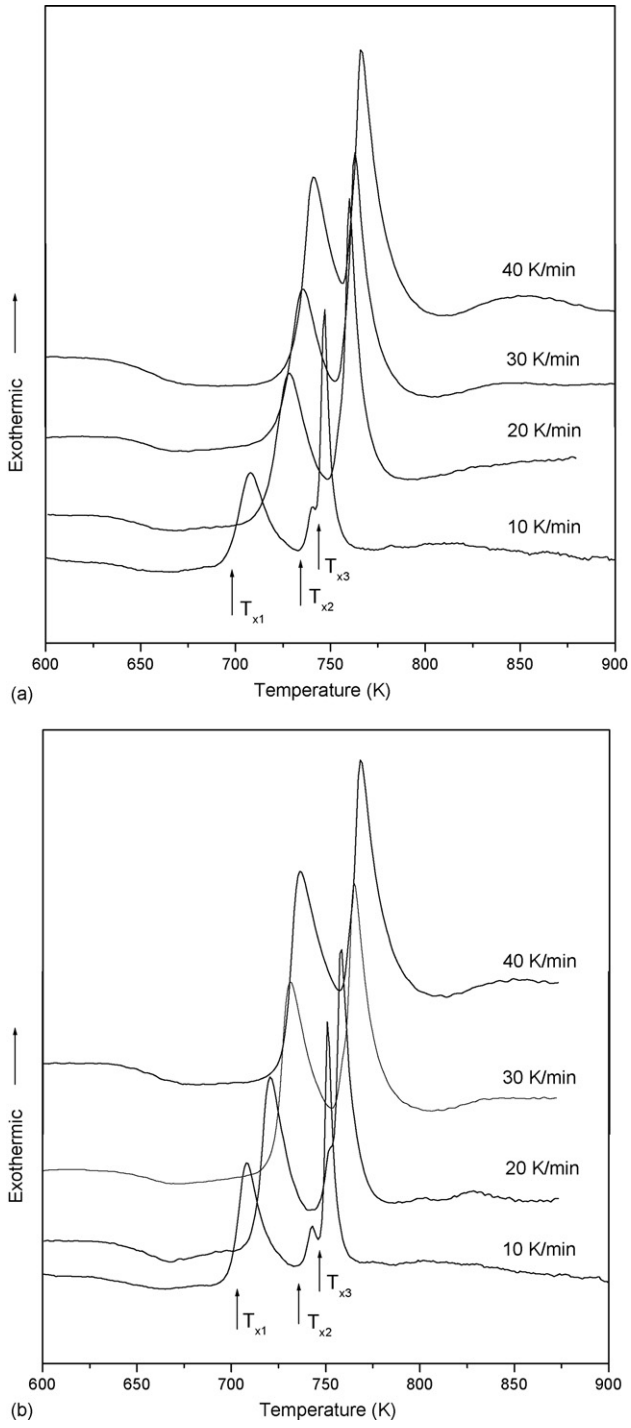


Fig. 4. DSC curves of the glasses G0 (a) and G12 (b) recorded at different scanning rates.

which is the characteristic of glass transition, followed by three exothermic events corresponding to crystallization reactions. These thermal behaviors agree with the results of Chen et al. [20]. The second exothermic peak can only be seen in the DSC plots at relatively low scanning rates, i.e., less than 10 K/min. As the scanning rate increases, the second and third exothermic peaks overlap. The first exothermic peak is verified to correspond to the AI phase transformation by XRD patterns of the annealed sample G0 at 673 K for 60 min (Fig. 5). As the specimens are heated

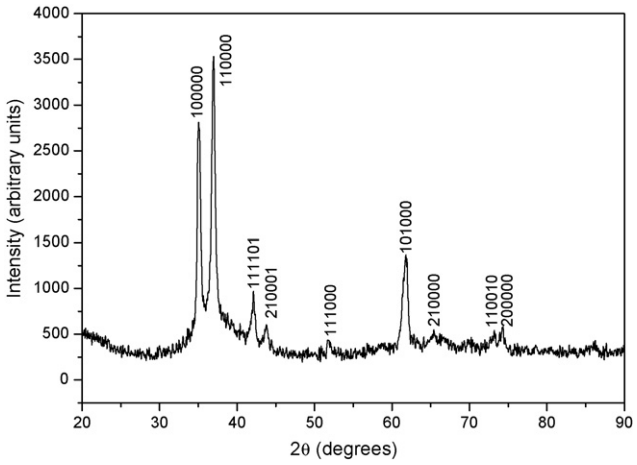


Fig. 5. XRD pattern of the glass G0 annealed at 673 K for 60 min.

beyond $T_{x1}$ continuously, the residual amorphous phase ($T_{x2}$) and I-phase ($T_{x3}$) begin to decompose into stable phases, such as $CuZr_2$- and $NiZr_2$-like ones [20]. Because of the overlapping of $T_{x2}$ and $T_{x3}$, the stability of the I-phase against decomposition can be evaluated by the value of $\Delta T_{x12}$ defined as the temperature span between $T_{x1}$ and $T_{x2}$. Under the same scanning rate, the values of $\Delta T_{x12}$ of G12 is larger than that of G0, which indicates that I-phase precipitated in the sample G12 is more stable against decomposition. The detailed discussion can be seen in the reference [21]. The effective activation energy for the AI phase transformation can be evaluated by Kissinger equation [22]:

$$\ln\frac{T^2}{\beta} = \frac{E}{RT} + C \quad (1)$$

where $T$ stands for the onset temperature of the formation of I-phase $T_{x1}$ and $\beta$ is the heating rate and $R$ the gas constant. The Kissinger plots $\ln(\beta/T^2)$ versus $1/T$ for the AI phase transformation of the glasses G0 and G12 are shown in Fig. 6.

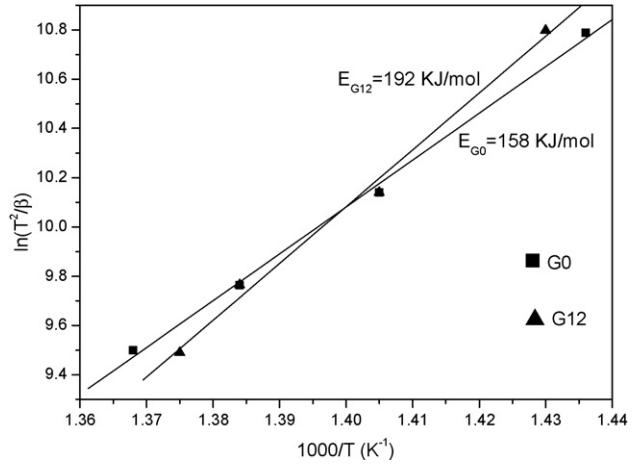


Fig. 6. Kissinger plots for the amorphous-to-icosahedral phase transformation of glasses G0 and G12. The effective activation energies for the transformation of the glasses G0 ($E_{G0}$) and G12 ($E_{G12}$) can be calculated by the slopes of Kissinger plots. $T$ stands for the onset temperature of the formation of I-phase $T_{x1}$.

The effective activation energy for the AI transformation in G12 ($E_{G12}$) is 192 kJ/mol, being larger than the value of G0 ($E_{G0}$ = 158 kJ/mol). Namely, the thermal stability of the amorphous sample G12 against formation of I-phase is higher than that of the sample G0, which agrees with the change of $\Delta T_{x12}$. The effective activation energies for AI phase transformation are much smaller than that for the transformation from amorphous to the stable $CuZr_2$- and $NiZr_2$-like phases (about 356 kJ/mol [23]). This indicates that the structure of I-phase is more similar to the amorphous matrix.

### 3.3. Transformation kinetics under isothermal conditions

The isothermal phase transformation of the glasses G0 and G12 in the supercooled liquid region (at 683, 688, 693 and 698 K) was investigated by DSC. The DSC curves exhibit a sharp exothermic peak, followed by two very gentle exothermic peaks. The first sharp exothermic peak corresponds to the AI phase transformation. The interest of this work is to investigate the kinetic mechanism of the AI phase transformation. Therefore, only the isothermal DSC traces of the first exothermic peaks are shown in Fig. 7. The detailed isothermal DSC data of the glasses G0 and G12 are shown in Tables 3 and 4, respectively.

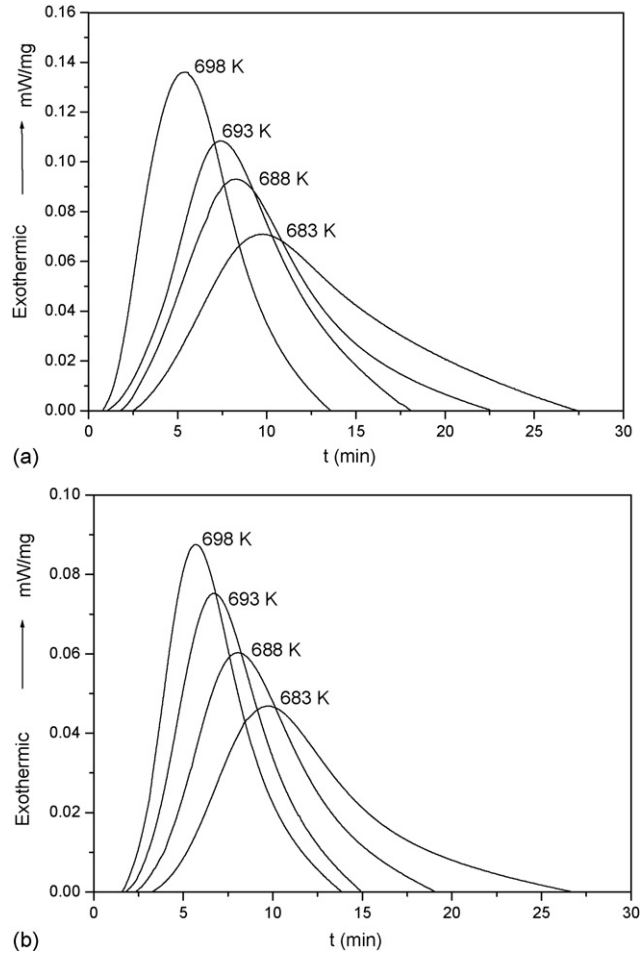


Fig. 7. The first exothermic peaks of isothermal DSC plots of the glasses G0 (a) and G12 (b) at different annealing temperatures.

Table 3
Isothermal kinetic parameters for amorphous-to-icosahedral phase transformation in the glass G0 at different annealing temperatures

| | Annealing temperature (K) | | | |
|---|---|---|---|---|
| | 683 | 688 | 693 | 698 |
| Incubation time, $\tau$ (min) | 4.05 | 3.12 | 2.52 | 1.77 |
| Avrami exponent, $n$ | 1.74 | 1.89 | 2.00 | 1.91 |
| Reaction constant, $k$ (min$^{-1}$) | 0.10 | 0.13 | 0.15 | 0.20 |
| Reaction peak width, $t_{95\%}$–$t_{1\%}$ (min) | 17.69 | 14.04 | 11.80 | 8.65 |

With the assumption that the precipitated volume fraction $x$ of I-phase, up to any time $t$, is proportional to the corresponding partial area of the exothermic peak, the volume fraction of I-phase with the transformation time can be evaluated by measuring the partial area of the exothermic peak. The results at different annealing temperatures are shown in Fig. 8. Their shapes are typical sigmoid. The TEM images of the glasses annealed at 673 K for 60 min show that spherical quasicrystals precipitate (Fig. 9), which further verifies the validity of the Johnson–Mehl–Avrami (JMA) equation to the AI phase transformation [24,25]. Based on the facts above, the AI phase transformation can be modeled by JMA equation as following [26,27]:

$$x(t) = 1 - \exp\{-[k(t-\tau)]^n\} \quad (2)$$

where $x(t)$ is the precipitated volume fraction, $t$ the annealing time, $\tau$ the incubation time, $n$ (called as Avrami exponent) a constant related to the behaviors of nucleation and growth during phase transformation and $k$ is the reaction rate constant.

Based on Eq. (2), the following equation can be obtained

$$\ln[-\ln(1-x)] = n\ln k + n\ln(t-\tau) \quad (3)$$

According to Eq. (3), the JMA plots at different annealing temperatures can be obtained by plotting $\ln[-\ln(1-x)]$ versus $\ln(t-\tau)$ using the data of $x = 15$–$85\%$ (Fig. 10). These JMA plots are nearly straight lines. The Avrami exponents $n$ and the reaction rate constants $k$ can be calculated by the slopes and intercepts of these JMA lines. The detailed results are shown in Tables 3 and 4.

Table 4
Isothermal kinetic parameters for amorphous-to-icosahedral phase transformation in the glass G12 at different annealing temperatures

| | Annealing temperature (K) | | | |
|---|---|---|---|---|
| | 683 | 688 | 693 | 698 |
| Incubation time, $\tau$ (min) | 4.75 | 3.64 | 2.97 | 2.49 |
| Avrami exponent, $n$ | 1.71 | 1.97 | 2.04 | 1.98 |
| Reaction constant, $k$ (min$^{-1}$) | 0.12 | 0.16 | 0.19 | 0.22 |
| Reaction peak width, $t_{95\%}$–$t_{1\%}$ (min) | 15.96 | 11.37 | 8.96 | 8.21 |

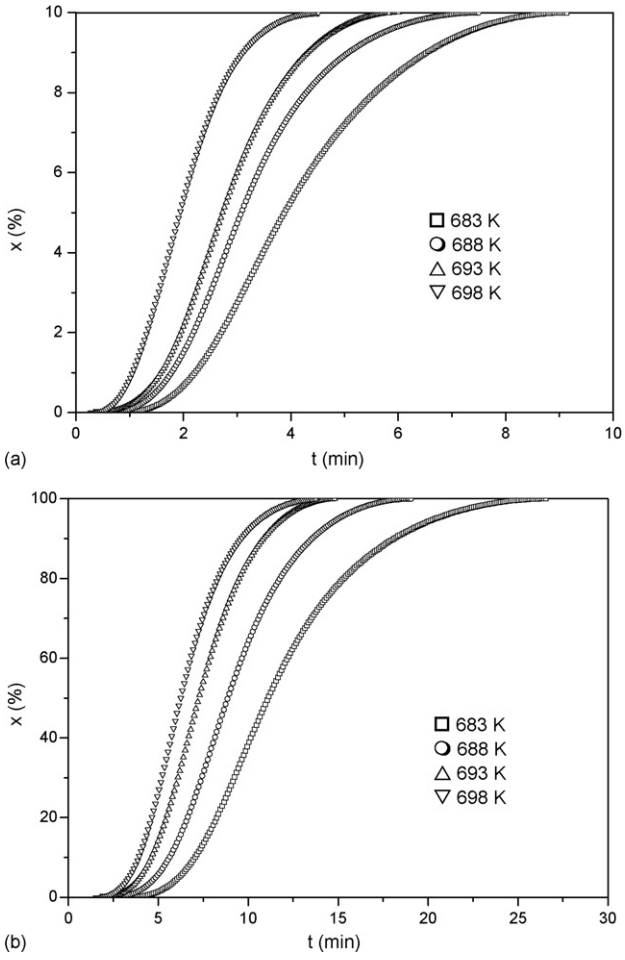


Fig. 8. Precipitated volume fraction of icosahedral quasicrystals as a function of annealing time in the glasses G0 (a) and G12 (b) at different annealing temperatures.

## 4. Discussion

### 4.1. Correlation between the solidification microstructure and the short-range order regions

When a solid is melted, the liquid appears to retain a "memory" of the solid structure [28]. As a result, the characteristic of solid state is reserved above the melting point in small regions, forming the melting boundary between the order regions and the surrounding amorphous ones. With the rise of liquid temperature, the melting front gradually penetrates into smaller order regions and more atoms are fused into amorphous regions. These order regions inherited from the solid state in a liquid are frozen as SRORs in the amorphous structure during the subsequent quenching. It should be emphasized that the atomic configuration of the SRORs may change during the melting and superheating processing of an alloy. Up to a critical temperature, above which the liquid becomes a true solution with homogenous distribution of atoms, the higher the liquid temperature is, the smaller the average size of SRORs in the liquid is [29]. Thus, the average size of SRORs in the $Zr_{65}Al_{7.5}Ni_{10}Cu_{12.5}Ag_5$ liquid at 1580 K is much smaller than that at 1300 K. After the subse-

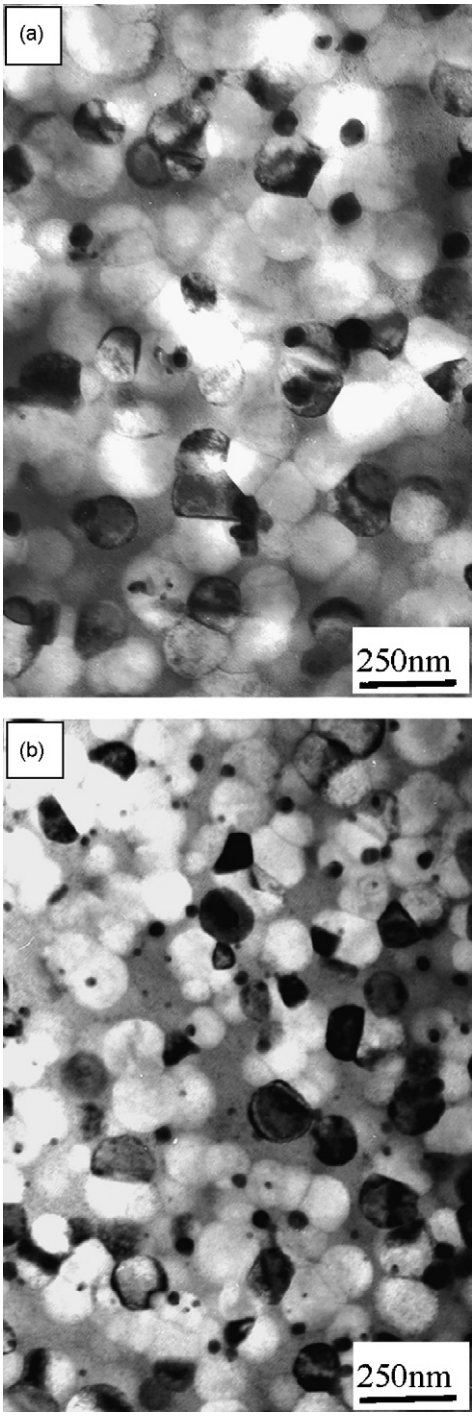


Fig. 9. TEM images of the spherical quasicrystals precipitated from the glasses G0 (a) and G12 (b) annealed at 720 K for 60 min.

quent solidification, the solidification microstructure of the ingot A12 is much finer than A0 due to structure heredity.

When the mother ingots are remelted to the casting temperature (about 1300 K), the average size of SRORs in the liquid A12 is much smaller than that in the liquid A0 since the structures of liquids have heredity to that of them. After the subsequent suction casting, the liquid structures are "frozen" into the corresponding amorphous structures. It is reasonable that the average size of SRORs in the as-cast sample G12 is much smaller than

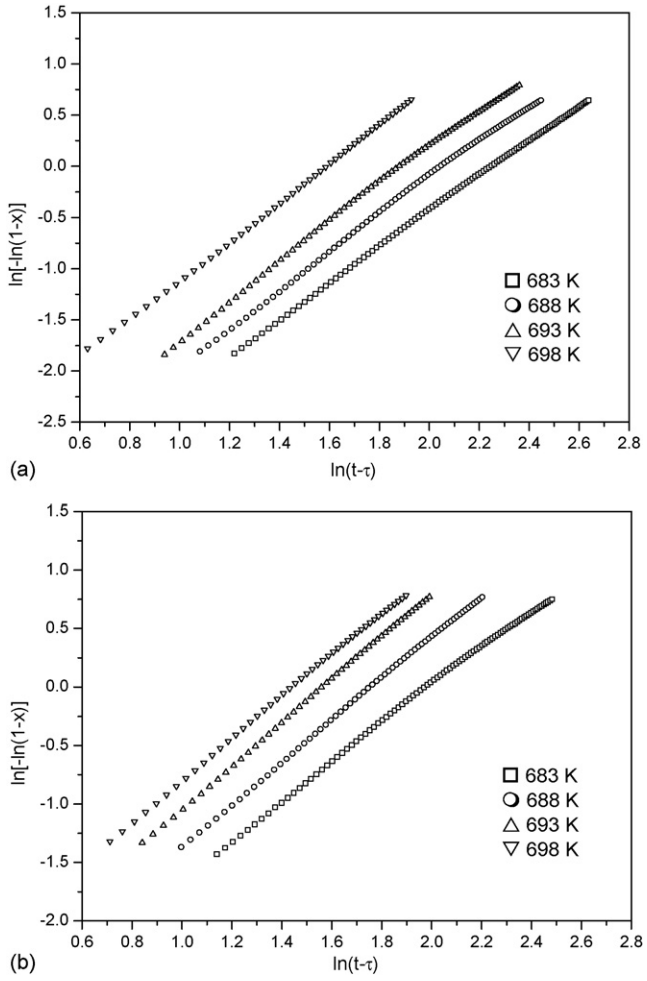


Fig. 10. JMA plots of the amorphous-to-icosahedral phase transformation of the glasses G0 (a) and G12 (b) at different annealing temperatures.

that in G0 (Fig. 3). This difference of the SRORs affects the crystallization kinetics, by which some information on the atomic configuration of the SRORs is hoped to be derived.

### *4.2. Mechanism of the transformation from amorphous to icosahedral phase*

The AI phase transformation in a Zr–Al–Ni–Cu–Ag metallic glass annealed at 663 K for various time has been investigated by monitoring the quasilattice constant and the compositions of quasicrystals [30]. It has been found that the quasilattice constant decreases with annealing time and the contents of Zr and Ag in the quasicrystals differ from those in the remaining amorphous matrix, which suggests that the AI phase transformation in the Zr–Al–Cu–Ni–Ag metallic glass is a reaction involving atomic diffusion [30]. All the Avrami exponents $n$ in the transformation of the glasses G0 and G12 are nearly a constant of 1.8 (Tables 3 and 4) within the experimental errors, which implies that the mechanism of the AI phase transformation does not change and that the formation of the quasicrystals is triggered by the growth of those SRORs act as the pre-exiting embryos [31]. The results support the argument that the SRORs in the amorphous structure have the icosahedron-like configuration.

### 4.3. Influence of the short-range order regions on the transformation kinetics

The incubation times and the effective activation energies for the AI phase transformation in the glasses G0 and G12 show that the formation of I-phase becomes more difficult as the average size of SRORs decreases. The effective activation energy for crystallization can be conceived as a weighted sum of the activation energies for nucleation and growth [32]. In the case of AI phase transformation of $Zr_{65}Al_{7.5}Ni_{10}Cu_{12.5}Ag_5$ amorphous alloy, the activation energy nearly all originates from that for growth since the AI phase transformation is activated by the diffusion of atoms that will adhere onto the surfaces of pre-existing SRORs. Experimental results have indicated that the underlying atomic diffusion mechanism in the supercooled metallic liquids is thermally activated collective hopping [33–35]. So, it can be assumed that the growth of the pre-existing SRORs in the $Zr_{65}Al_{7.5}Ni_{10}Cu_{12.5}Ag_5$ glass is mainly dominated by the movement of atomic groups, during which the redistribution of atoms involves. The more uniform the distribution of atoms in the metallic glass is, the more work for the redistribution of atoms is needed, which contributes to the larger effective activation energy for AI phase transformation and longer incubation period in the glass G12.

The Avrami exponent of the AI phase transformation does not change with the variation of the states of the SRORs in the $Zr_{65}Al_{7.5}Ni_{10}Cu_{12.5}Ag_5$ glass, indicating that the size of SRORs has little influence on the mechanism of AI phase transformation. But the difference of SRORs results in the change of crystallization rate. At the same annealing temperature, the glass G12 exhibits a narrower reaction peak width ($t_{95\%}$–$t_{1\%}$) and a higher reaction constant $k$ (Tables 3 and 4), which suggests that the transformation rate in the glass G12 is quicker than that of glass G0. Compared with the annealed sample G0 (about 180 nm), the average size of the quasicrystals in the annealed glass G12 (about 100 nm) is smaller, but the number per unit volume is larger (Fig. 9). If it is assumed that those SRORs in the amorphous matrix act as the pre-existing embryos of I-phase during the crystallization, it is reasonable to suggest that the density of the SRORs per unit volume in the glass G12 is larger than that in the glass G0. Once the crystallization is activated, the probability of amorphous atoms to adhere onto the growing embryos (SRORs) in the glass G12 is larger than that in glass G0. Therefore, the number of atoms captured by the growing quasicrystals (SRORs) per unit volume and per unit time in the glass G12 is larger than that of the glass G0, resulting in a higher transformation rate in the glass G12. This change of the phase transformation rate further indicates that the pre-existing SRORs in the metallic glass, without structure readjustment, do act as embryos for icosahedral quasicrystals. In other words, the SRORs in the metallic glass show an icosahedron-like atomic configuration.

## 5. Conclusions

After the repeated arc melting at 1580 K, the solidification microstructure of the $Zr_{65}Al_{7.5}Cu_{12.5}Ni_{10}Ag_5$ ingot is considerably refined. Due to the structure heredity, the average size of SRORs in the sample prepared from ingot with finer microstructure is considerably smaller. Kinetic analyses reveal that the effective activation energy for the AI phase transformation increases as the average size of SRORs decreases, indicating an enhancement of the thermal stability against crystallization. The value of the Avrami exponent is nearly a constant of 1.8 although the average size of SRORs changes, which indicates that those SRORs in the metallic glass act as the pre-existing embryos of the icosahedral quasicrystals, namely, the SRORs show an icosahedron-like atomic configuration. The finer solidification microstructure gives rise to the increase of the SRORs in the corresponding amorphous structure, leading to the increase of the net flux of atoms from the amorphous matrix to the growing quasicrystals during crystallization. As a result, an unexpected rise of transformation rate occurs.

## Acknowledgements

The authors are grateful to the financial support of the Natural Science Foundation of Shanxi Province, China (Grant No. 20051032), the Shanxi Provincial Foundation for Leaders of Disciplines in Science and the Doctoral Science Foundation of Taiyuan University of Science and Technology. The authors express thanks to Dr. Q.P. Cao for his kind help of DSC experiments.

## References

[1] P. Chaudhari, D. Turnbull, Science 11 (1978) 199.
[2] D.R. Nelson, B.I. Halperin, Science 229 (1985) 233.
[3] Y.T. Cheng, W.L. Johnson, Science 235 (1987) 997.
[4] A.L. Greer, Science 267 (1995) 1947.
[5] A. Inoue, Acta Mater. 48 (2000) 279.
[6] H.S. Chen, Rep. Prog. Phys. 43 (1980) 353.
[7] D. Shechtman, I. Blech, D. Gratias, J.W. Cahn, Phys. Rev. Lett. 53 (1984) 1951.
[8] P.J. Steinhart, D.R. Nelson, M. Ronchetti, Phys. Rev. B 28 (1984) 784.
[9] H. Jónsson, H.C. Andersen, Phys. Rev. Lett. 60 (1988) 2295.
[10] F.H. Stillinger, Science 267 (1995) 1935.
[11] H. Reichert, O. Klein, H. Dosch, M. Denk, V. Honkimäki, T. Lippmann, G. Reiter, Nature 408 (2000) 839.
[12] W.K. Luo, H.W. Sheng, F.M. Alamgir, J.M. Bai, J.H. He, E. Ma, Phys. Rev. Lett. 92 (2004) 145502.
[13] J. Saida, M. Matsushita, A. Inoue, Appl. Phys. Lett. 79 (2001) 412.
[14] K. Saksl, H. Franz, P. Jóvári, K. Klementiev, E. Welter, A. Ehnes, J. Saida, A. Inoue, J.Z. Jiang, Appl. Phys. Lett. 83 (2003) 3924.
[15] J. Saida, M. Matsushita, T. Zhang, A. Inoue, M.W. Chen, T. Sakurai, Appl. Phys. Lett. 75 (1999) 3497.
[16] L.C. Chen, F. Spaepen, Nature 336 (1988) 366.
[17] M.W. Chen, T. Zhang, A. Inoue, A. Sakai, T. Sakurai, Appl. Phys. Lett. 75 (1999) 1697.
[18] A. Inoue, T. Zhang, J. Saida, M. Matsushita, M.W. Chen, T. Sakurai, Mater. Tans. JIM 40 (1999) 1181.
[19] A. Inoue, J. Saida, M. Matsushita, T. Sakurai, Mater. Trans. JIM 41 (2000) 362.
[20] M.W. Chen, I. Dutta, T. Zhang, A. Inoue, T. Sakurai, Appl. Phys. Lett. 79 (2001) 42.
[21] Z.J. Yan, J.F. Li, S.R. He, H.H. Wang, Y.H. Zhou, Mater. Trans. 44 (2003) 907.
[22] H.E. Kissinger, Anal. Chem. 29 (1957) 1702.

[23] Z.J. Yan, J.F. Li, H.H. Wang, S.R. He, Y.H. Zhou, Sci. China Ser. E 46 (2003) 639.
[24] D.W. Henderson, J. Non-Cryst. Solids 30 (1979) 301.
[25] M.P. Shepilov, D.S. Baik, J. Non-Cryst. Solids 171 (1994) 141.
[26] M.A. Johnson, R.F. Mehl, Trans. Am. Inst. Min. Metall. Pet. Eng. 135 (1939) 416.
[27] M. Avrami, J. Chem. Phys. 9 (1941) 177.
[28] F.C. Frank, Proc. R. Soc. London A 215 (1952) 43.
[29] P.S. Popel, O.A. Chikova, V.M. Matveev, High Temp. Mater. Process. 4 (1995) 219.
[30] J.Z. Jiang, A.R. Rasmussen, C.H. Jensen, Y. Lin, P.L. Hansen, Appl. Phys. Lett. 80 (2002) 2090.
[31] J.W. Christian, The Theory of Transformation in Metals and Alloys, Pergamon, Oxford, UK, 1975.
[32] A.T.W. Kempen, F. Sommer, E.J. Mittemeijer, J. Mater. Sci. 37 (2002) 1321.
[33] X.P. Tang, U. Geyer, R. Busch, W.L. Johnson, Y. Wu, Nature 402 (1999) 160.
[34] W.H. Wang, L.L. Li, M.X. Pan, R.J. Wang, Phys. Rev. B 63 (2001) 052204.
[35] V. Zöllmer, K. Rätzke, F. Faupel, A. Rehmet, U. Geyer, Phys. Rev. B 65 (2002) 220201.